Supporting Information

A new mechanism for visible light photocatalysis: Generation of intraband by adsorbed organic compounds with wide-bandgap semiconductors

Teng Wang [a, #], *Jiachun Cao* [a, b #], *Juan Li* [b], *Juntian Li* [b], *Didi Li* [a], *Shaobin Wang* [c], *Zhimin Ao* [b, a*]

[a] Guangdong-Hong Kong-Macao Joint Laboratory for Contaminants Exposure and Health, Guangdong Key Laboratory of Environmental Catalysis and Health Risk Control, Key Laboratory for City Cluster Environmental Safety and Green Development of the Ministry of Education, Institute of Environmental Health and Pollution Control, School of Environmental Science and Engineering, Guangdong University of Technology, Guangzhou 510006, China

[b] Advanced Interdisciplinary Institute of Environment and Ecology, Beijing Normal University, Zhuhai 519087, China

[c] School of Chemical Engineering, The University of Adelaide, Adelaide, SA 5005, Australia.

[#] These authors contributed equally

[*] Corresponding authors: E-mail: zhimin.ao@bnu.edu.cn (ZA)

Pages - 24

Table - 5

Fig.s - 16

Table S1. The models and software parameters used in our surface calculations.

Type	Miller index	Terminate	Supercell	Reference	K-mesh	
					Relax	SCF
A-TiO_2	101	O-Ti-O	1 × 4 × 3	[1]	2 × 2 × 1	3 × 3 × 1
R-TiO_2	110	O-Ti-O	4 × 2 × 3	[2]	2 × 2 × 1	3 × 3 × 1
La_2O_3	001	La-O	2 × 3 × 2	[3]	2 × 2 × 1	2 × 3 × 1
Sb_2O_3	111	Sb-O, Sb	1 × 1 × 2	[4]	2 × 2 × 1	2 × 2 × 1

Table S2. Information on oxidation products of styrene by visible light photolysis of TiO_2 detected by PTR-ToF-MS.

Entry	m/z	Name	Formula	Reference
1	43.017	ketene	C_2H_2O	[5]
2	45.019	acetaldehyde	C_2H_4O	[5, 6]
3	47.044	ethanol	C_2H_6O	[5]
4	59.059	acetone	C_3H_6O	[5, 6]
5	61.063	acetic acid	$C_2H_4O_2$	[5, 6]
6	79.054	benzene	C_6H_6	[5, 6]
7	95.061	phenol	C_6H_6O	[5, 6]
8	105.067	styrene	C_8H_8	[5]

Table S3. The experimental and calculated CBM and VBM (eV).

	Exp.		Cal.		
	CBM	VBM	Miller index	CBM	VBM
A-TiO_2	-0.72	2.55	101	-0.62	2.56
R-TiO_2	-0.25	2.77	110	-0.17	2.78
La_2O_3	-3.39	2.74	001	-2.71	1.28
Sb_2O_3	-1.81	2.23	111	-1.74	1.68

Table S4. The experimental and calculated band gap energy (eV).

	Exp.	Cal.		
		U_{eff}	Bulk	Surface
A-TiO_2	3.27	7.5	3.24	3.18
R-TiO_2	3.02	9.5	3.02	2.94
La_2O_3	5.03	5.4	3.99	3.99
Sb_2O_3	4.04	4.5	3.38	3.43

Table S5. The adsorption energy (E_{ads}, eV) of VOC molecules on simulated surfaces.

	Styrene	Toluene	Benzene	Ethyl acetate
A-TiO_2 (101)	-1.021	-0.531	-0.692	-1.005
R-TiO_2 (110)	-1.087	-0.867	-0.747	-1.265
La_2O_3 (001)	-1.020	-0.977	-1.026	-1.046
Sb_2O_3 (111)	-0.566	-0.539	-0.526	-0.481

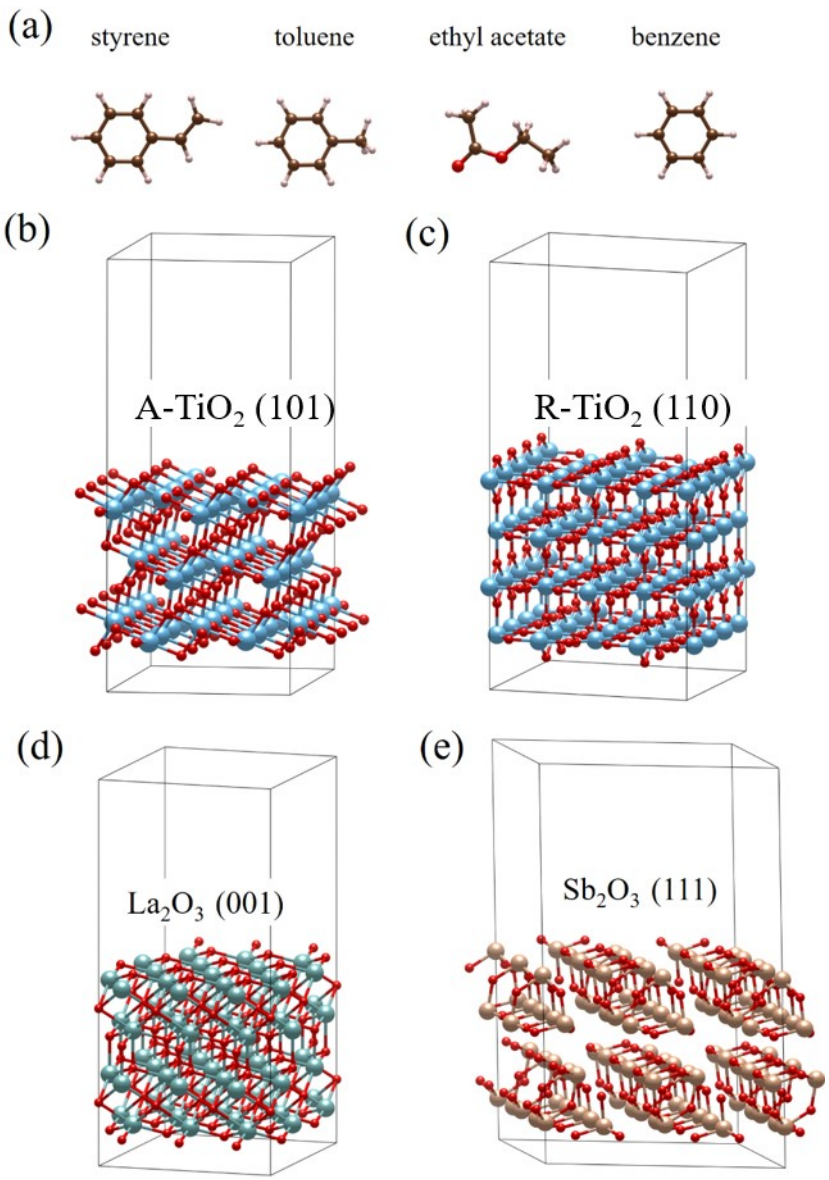

Fig. S1. The optimized structures of VOC molecules and semiconductor surfaces.

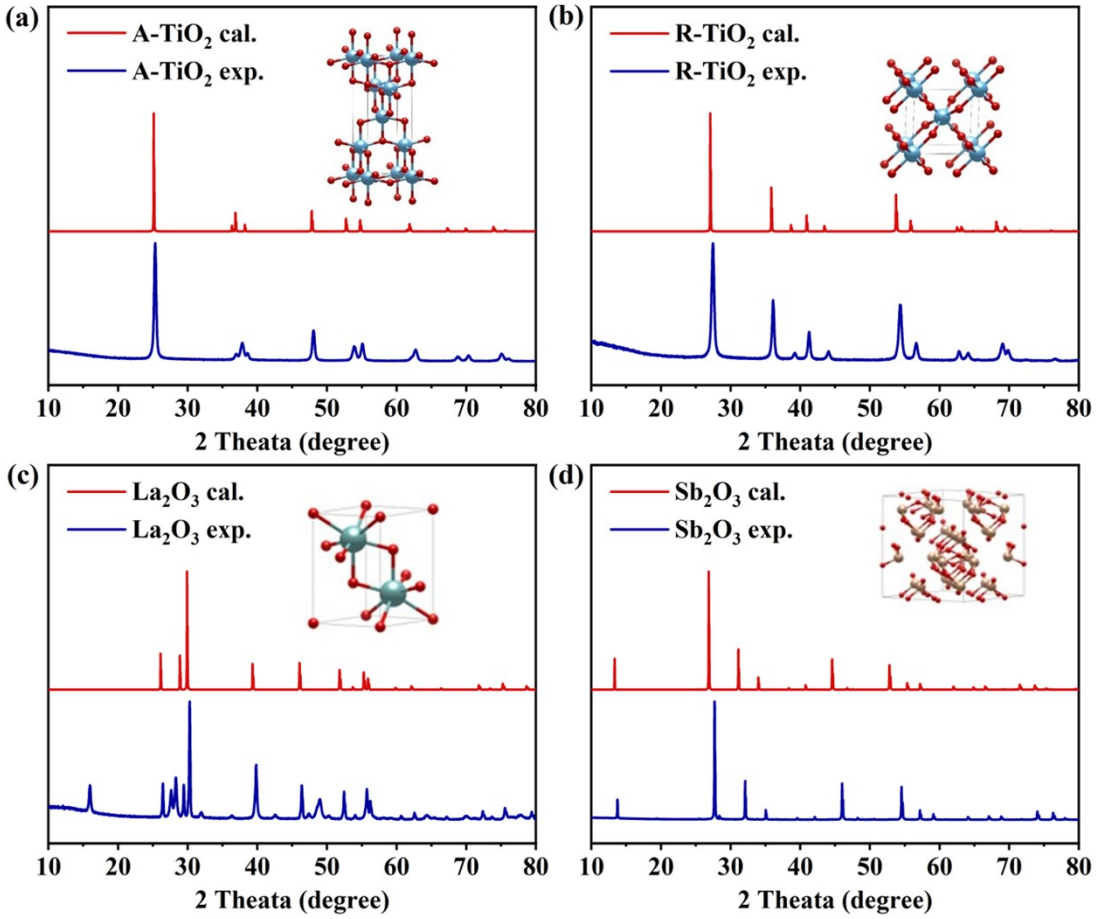

Fig. S2. Comparison of the experimental and calculated powder diffraction patterns of semiconductors.

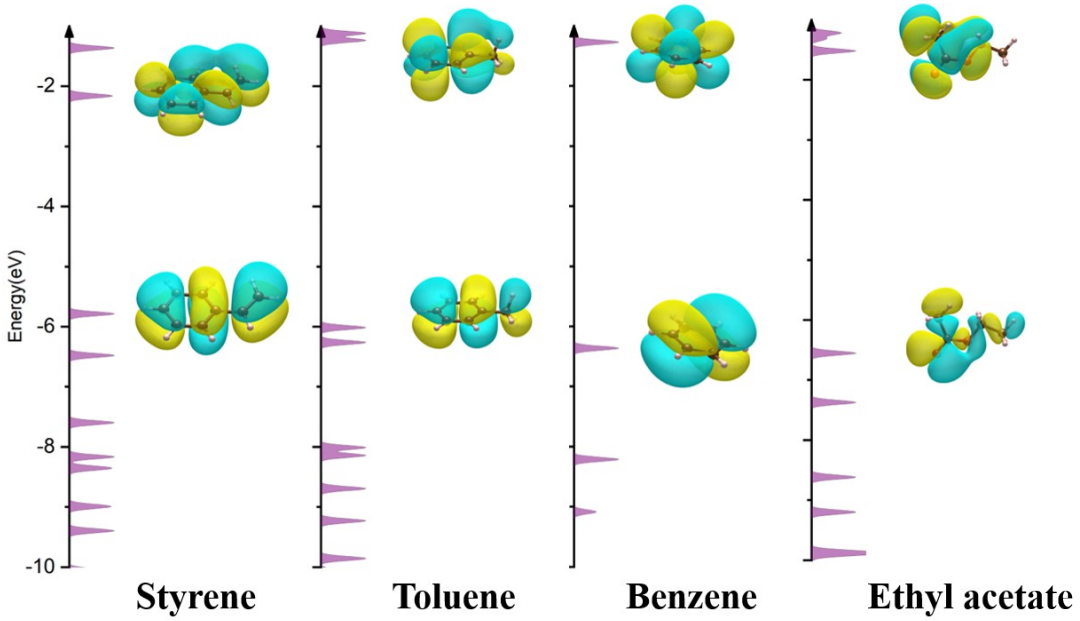

Fig. S3. DOS and charge distributions of front orbitals of VOC molecules in a vacuum state.

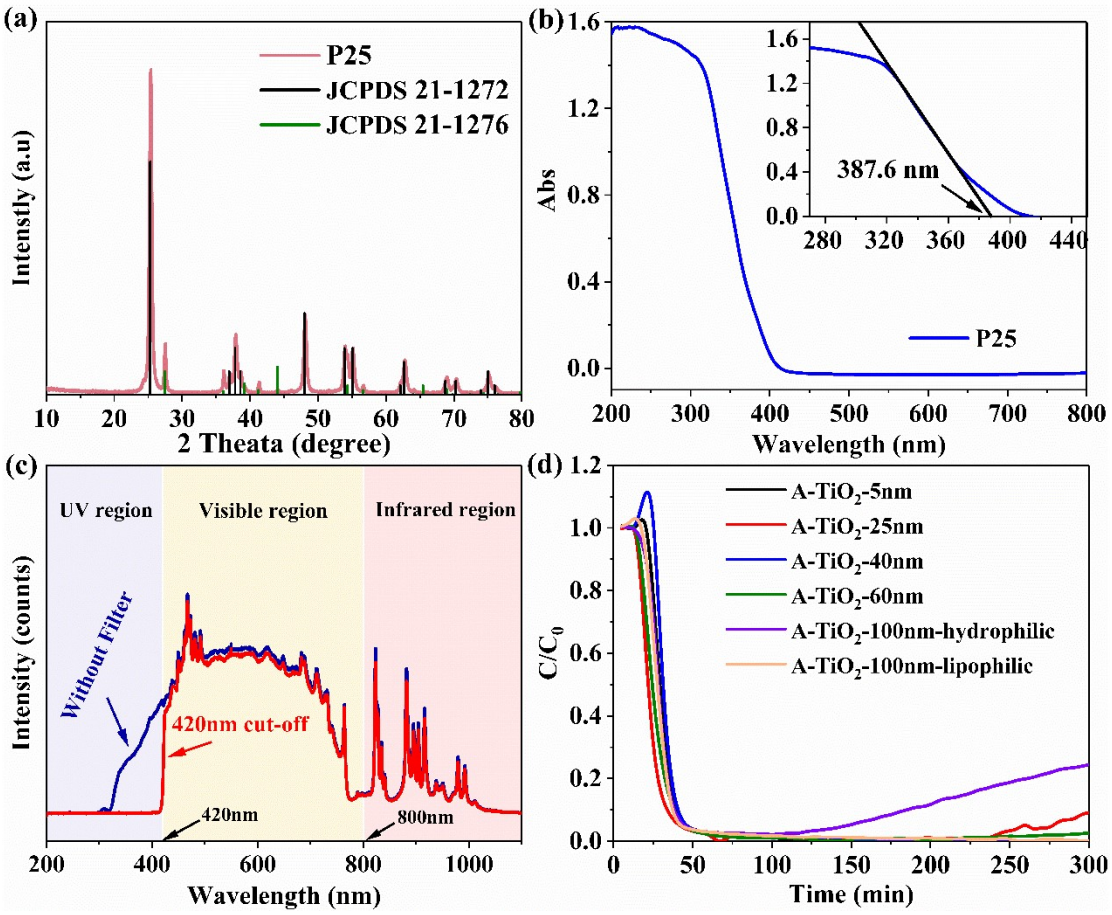

Fig. S4 (a) XRD spectra of P25 obtained in this work and from the PDF cards; (b) UV-Vis diffuse reflection absorption patterns and absorption band edges of P25; (c) The spectral distribution of the Xenon light source without a filter and with a Cut 420 filter; (d) Degradation curves of styrene by A-TiO_2 with different particle sizes.

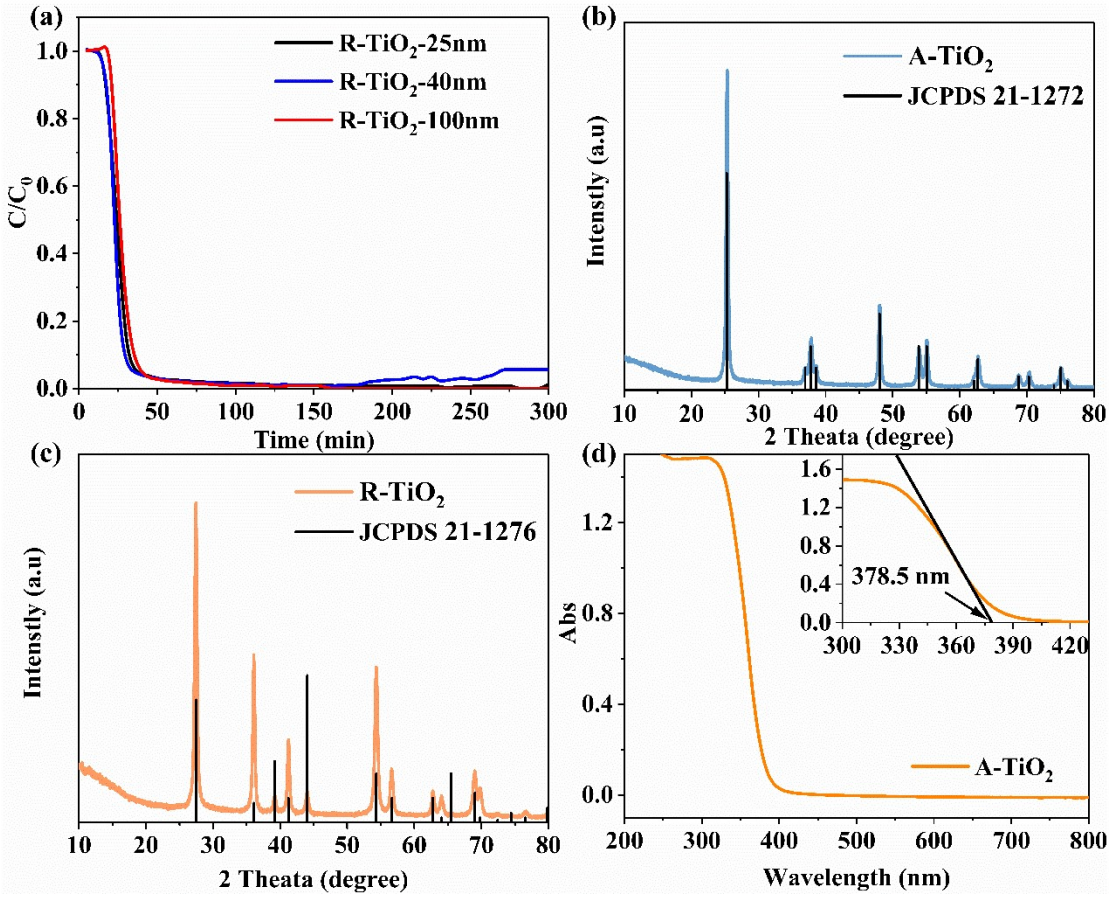

Fig. S5. (a) Degradation curves of styrene by R-TiO_2 with different particle sizes; XRD spectra of (b) A-TiO_2 and (c) R-TiO_2 obtained in this work and from the PDF cards; (d) UV-Vis diffuse reflection absorption patterns and absorption band edges of A-TiO_2.

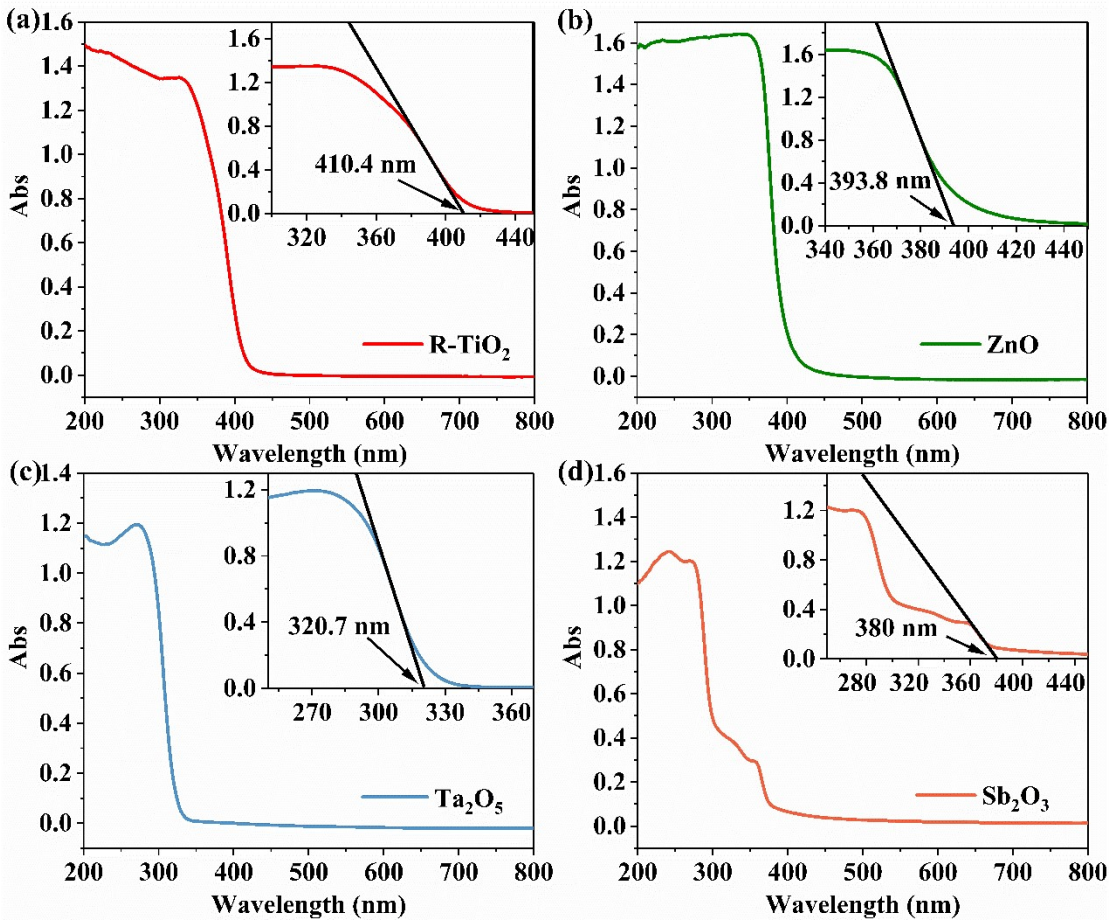

Fig. S6. UV-Vis diffuse reflection absorption patterns and absorption band edges of (a) R-TiO_2, (b) ZnO, (c) Ta_2O_5 and (d) Sb_2O_3.

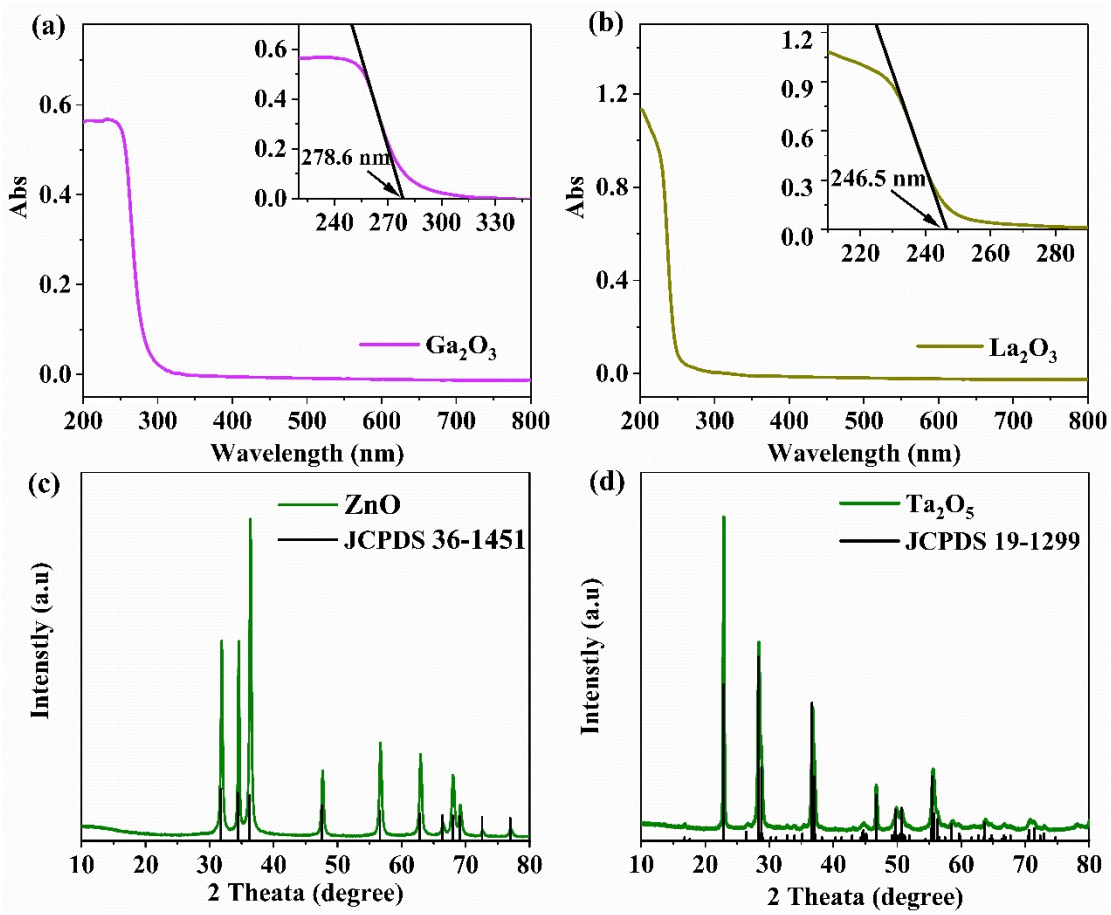

Fig. S7. UV-Vis diffuse reflection absorption patterns and absorption band edges of (a) Ga_2O_3 and (b) La_2O_3; XRD spectra of (c) ZnO and (d) Ta_2O_5 obtained in this work and from PDF cards.

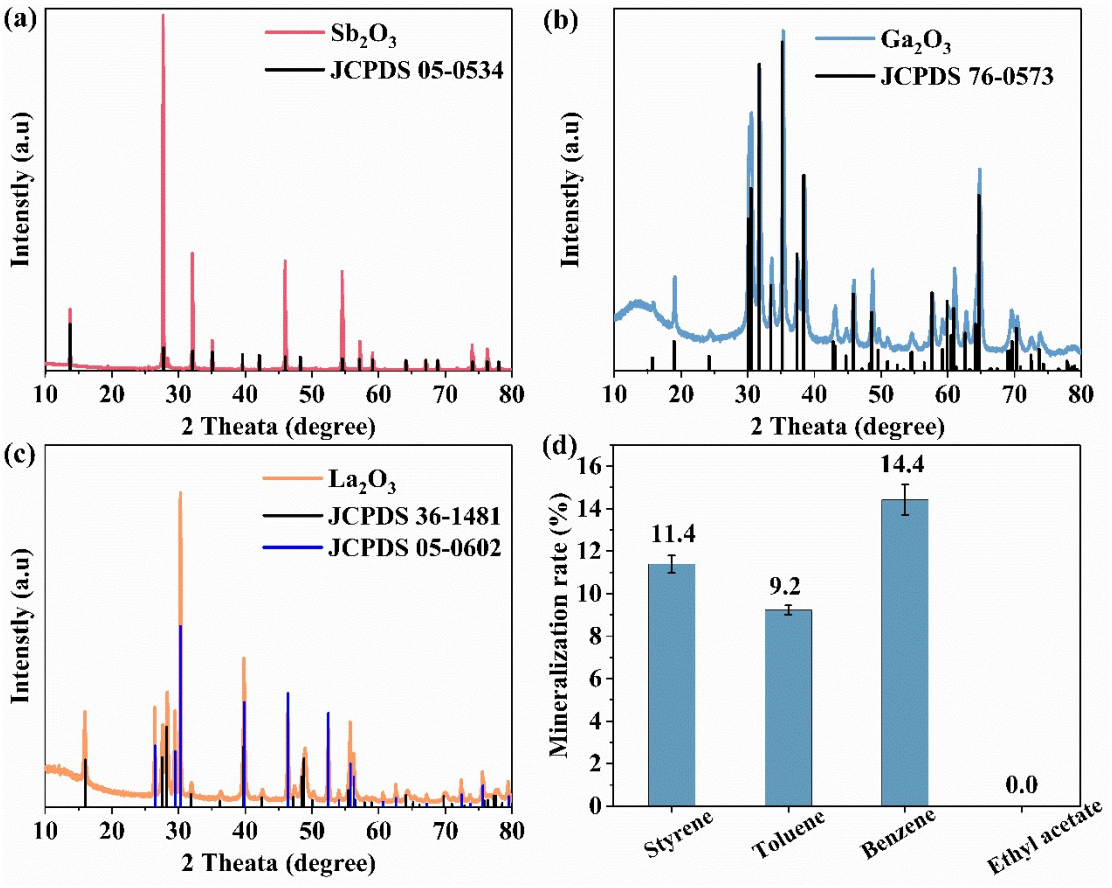

Fig. S8. XRD spectra of (a) Sb_2O_3, (b) Ga_2O_3 and (c) La_2O_3 obtained in this work and from PDF cards; (d) Histogram of the degradation mineralization rate of A-TiO_2 for different VOCs.

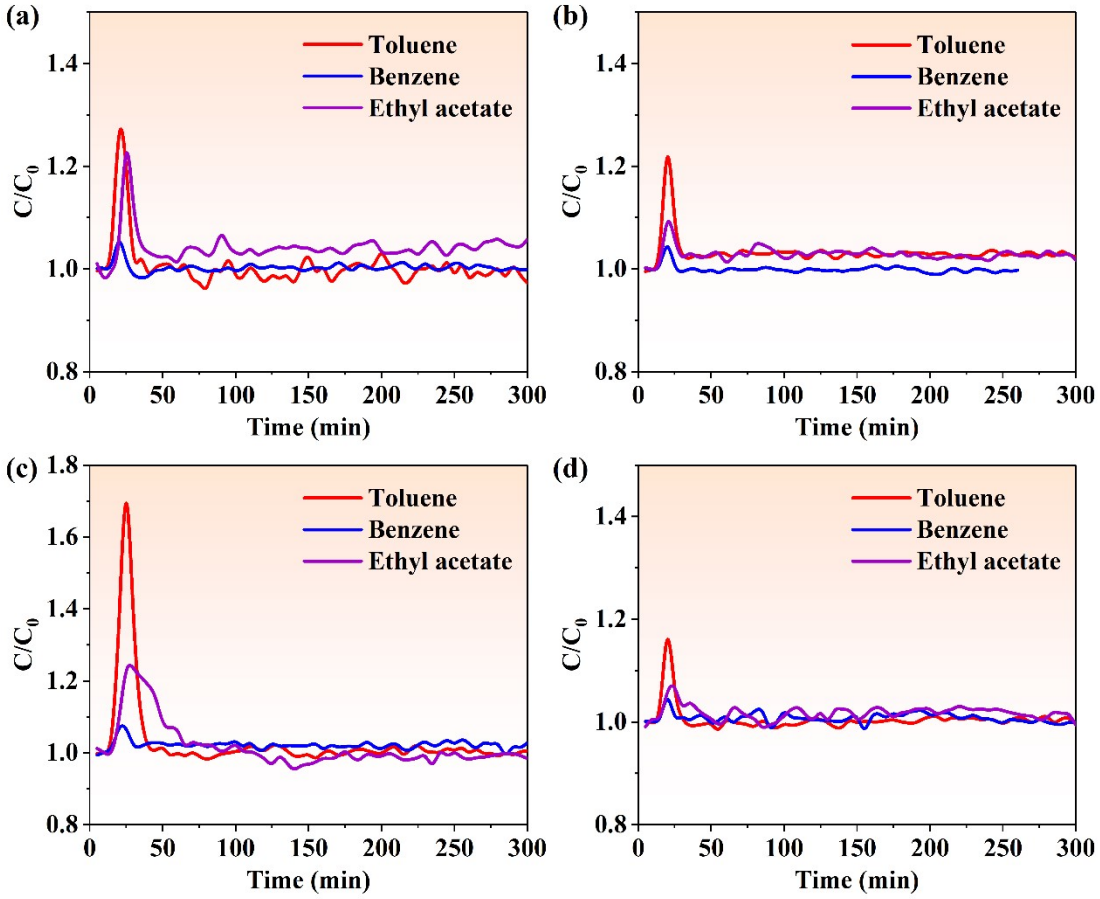

Fig. S9. Degradation curves of toluene, benzene and ethyl acetate by (a) Ta_2O_5, (b) Sb_2O_3, (c) Ga_2O_3 and (d) La_2O_3.

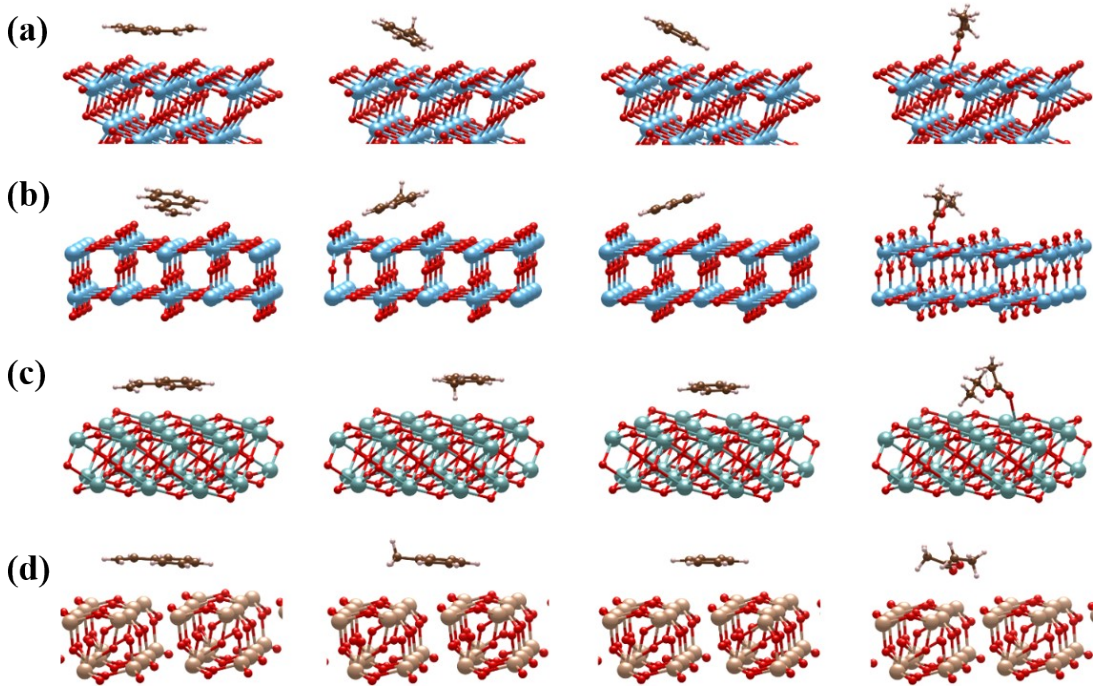

Fig. S10. The most stable adsorption configurations of styrene, toluene, benzene, and ethyl acetate on the simulated surfaces of (a) A-TiO_2, (b) R-TiO_2, (c) La_2O_3, and (d) Sb_2O_3, respectively.

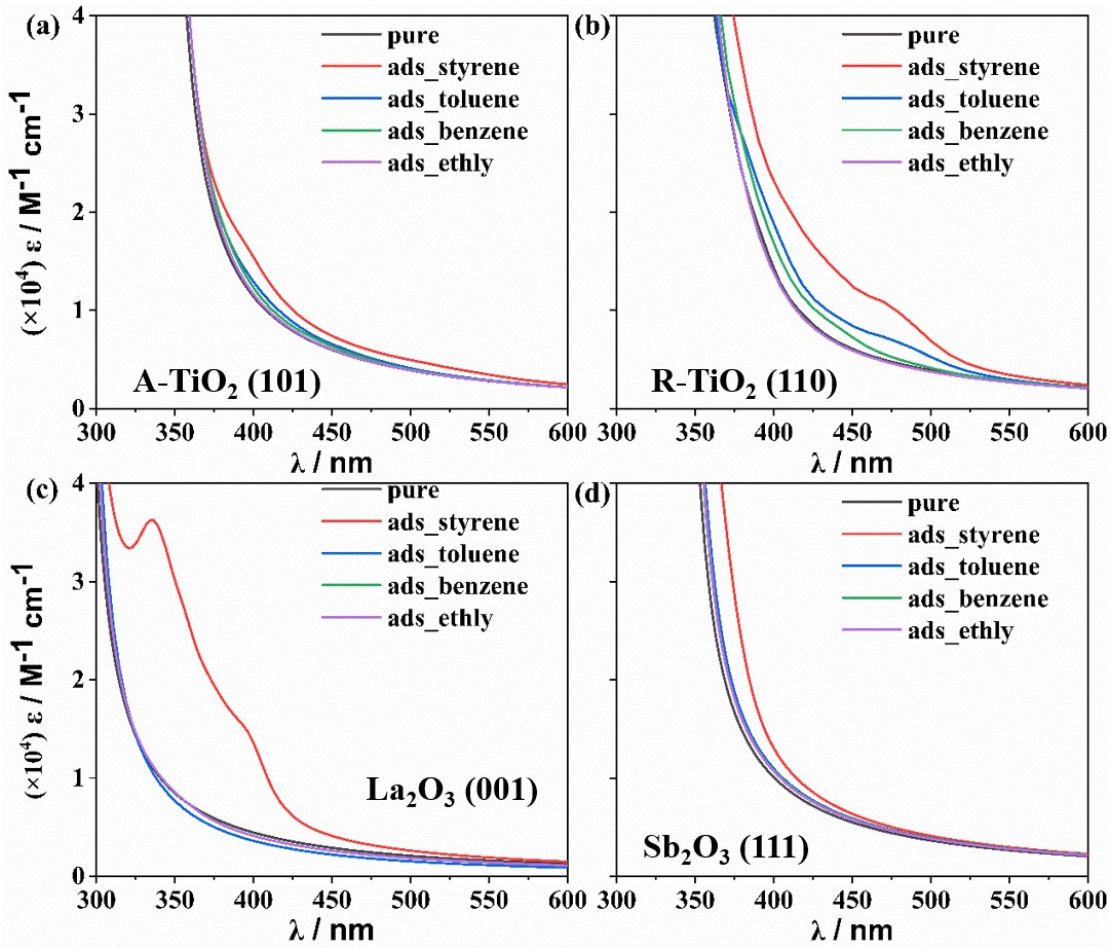

Fig. S11. Simulated absorption spectra of bare and modified semiconductor surfaces.

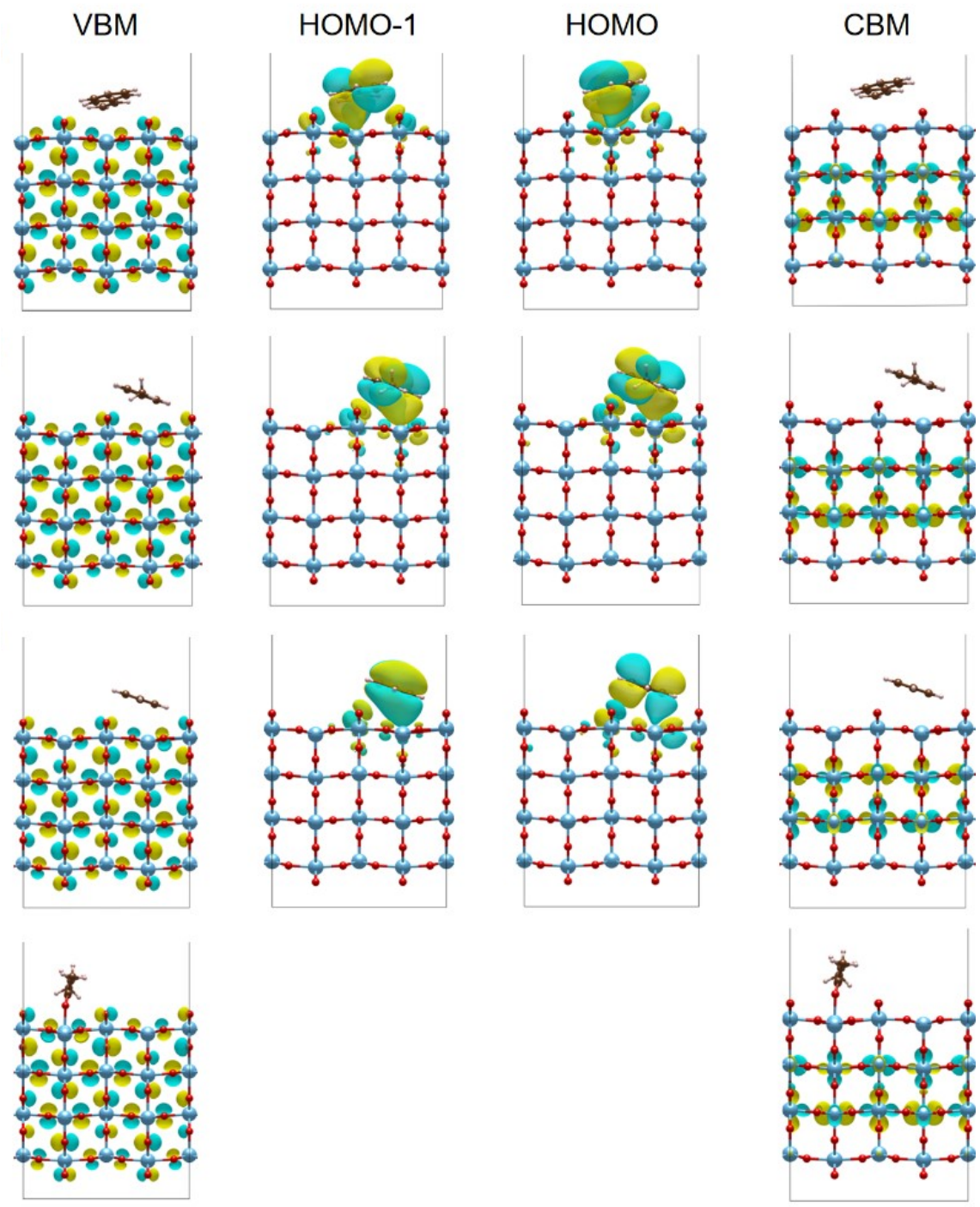

Fig. S12. The pivotal orbitals of A-TiO_2 (101) adsorption systems with adsorbing VOC molecules. VBM, CBM of semiconductor surfaces and molecule orbital exiting in the semiconductor band gap.

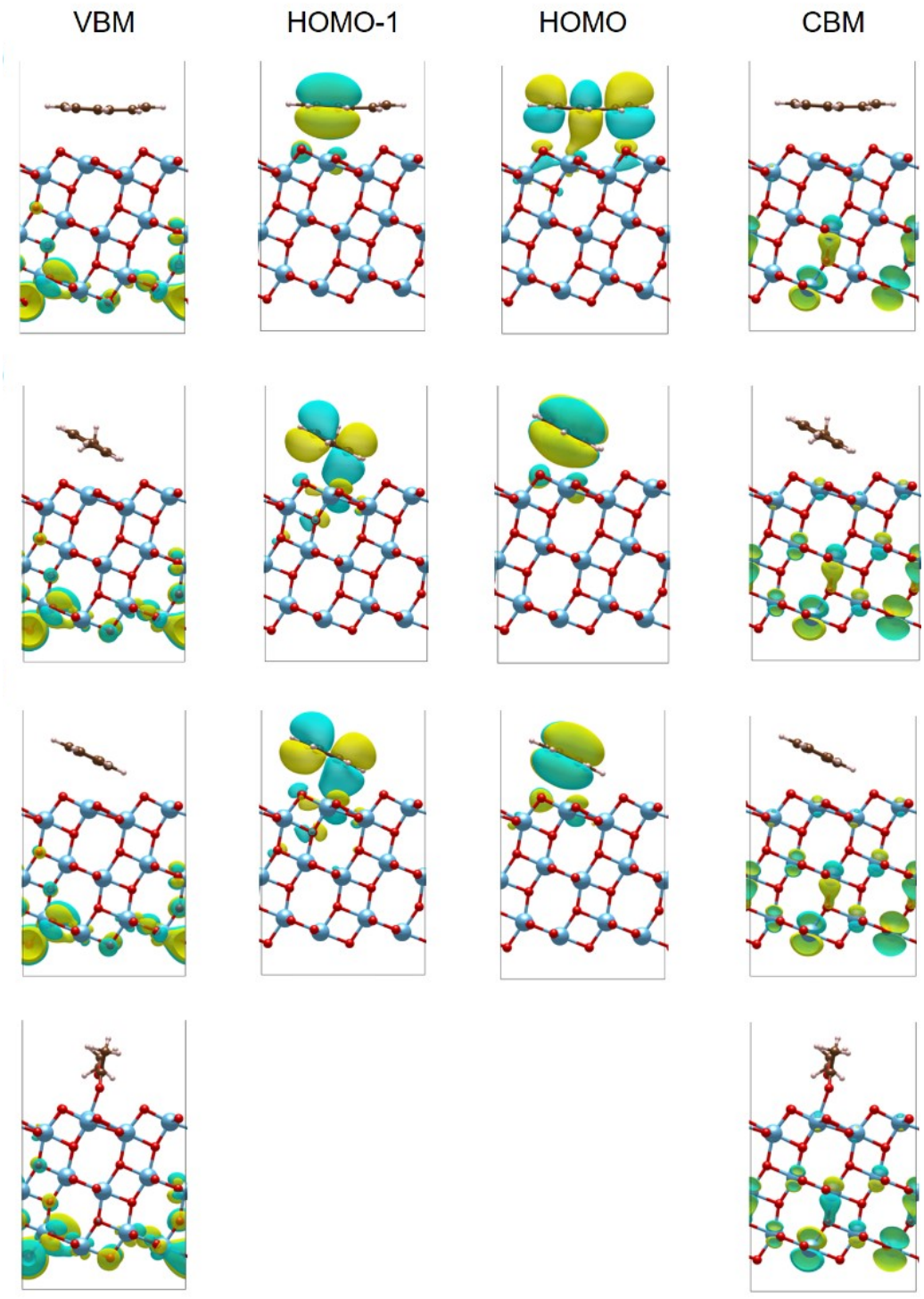

Fig. S13. The pivotal orbitals of R-TiO_2 (110) adsorption systems with adsorbing VOC molecules. VBM, CBM of semiconductor surfaces and molecule orbital exiting in the semiconductor band gap.

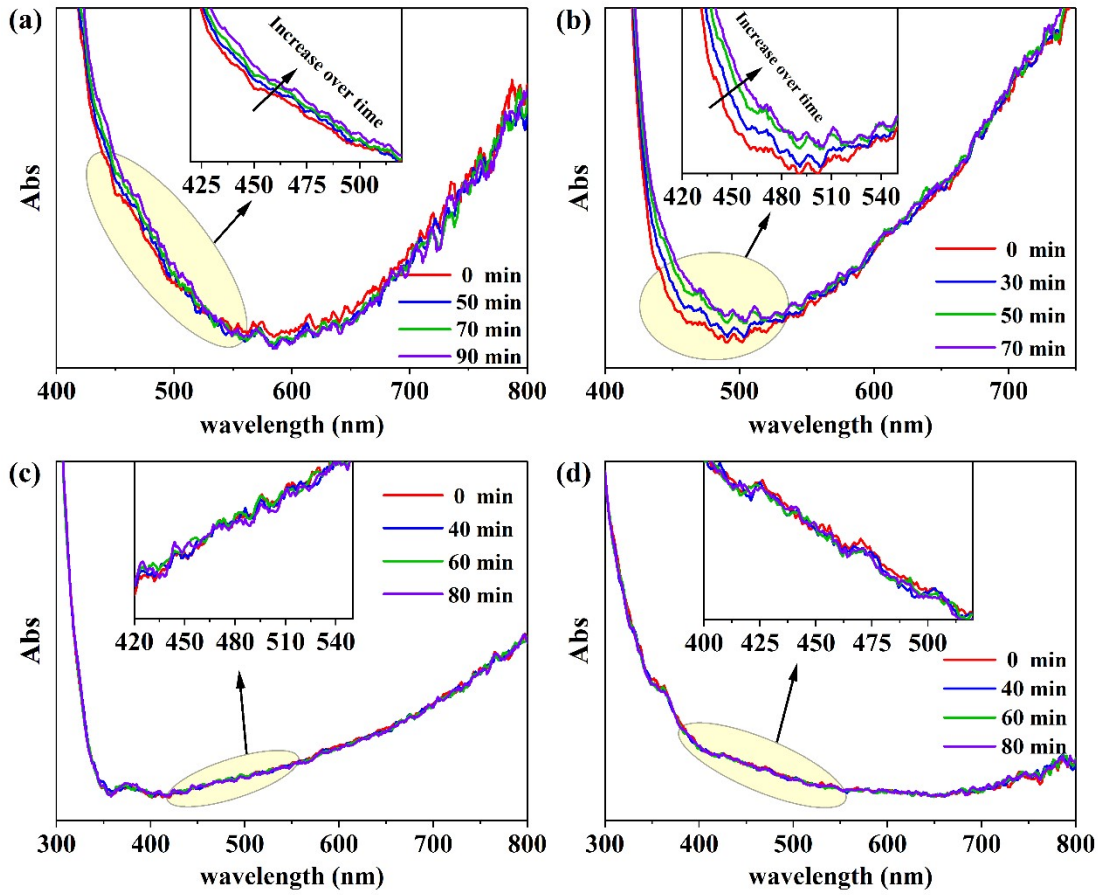

Fig. S14. *In situ* UV-Vis absorption spectra of (a) A-TiO_2, (b) P25, (c) Ga_2O_3 and (d) La_2O_3 during continuous adsorption of toluene.

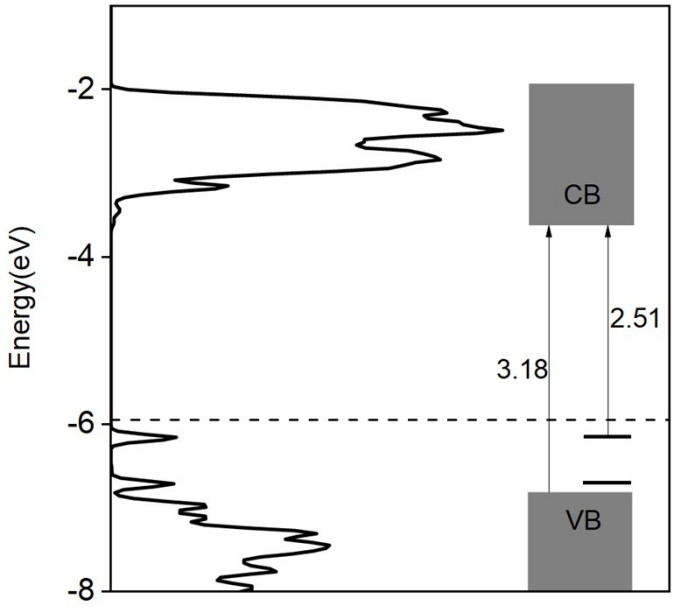

Fig. S15. DOS plot for phenol molecule adsorbed on A-TiO_2 (101) surface. The right end of the Fig. shows the position of the newly created midgap states in the electronic structure of the A-TiO_2 surface.

(a)

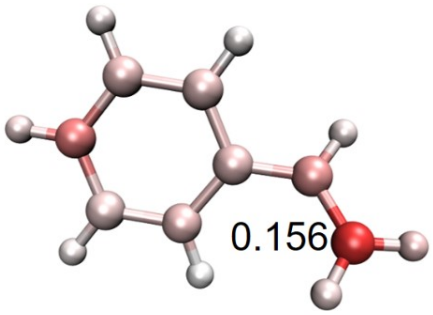

(b)

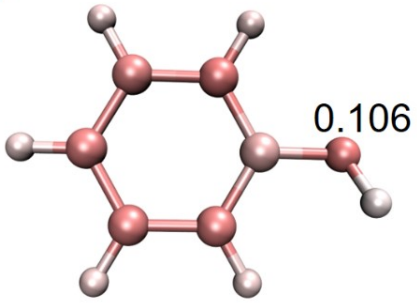

(c)

Styrene		
No.	Atom	f^-
1	C	0.061
2	C	0.063
3	C	0.059
4	C	0.054
5	C	0.062
6	C	0.106
7	C	0.088
8	C	0.156
9	H	0.032
10	H	0.036
11	H	0.039
12	H	0.041
13	H	0.050
14	H	0.043
15	H	0.049
16	H	0.060

Phenol		
No.	Atom	f^-
1	C	0.106
2	C	0.097
3	C	0.100
4	C	0.101
5	C	0.101
6	C	0.072
7	O	0.106
8	H	0.055
9	H	0.055
10	H	0.053
11	H	0.056
12	H	0.054
13	H	0.043

Fig. S16. Atomic structure of styrene (a) and phenol (b) colored according to Condemned Fukui function (f^-) data (c). The atom with a larger Fukui function (f^-) is colored redder.

References

1 Lamiel-Garcia O, Tosoni S, Illas F. Relative Stability of F-Covered TiO_2 Anatase (101) and (001) Surfaces from Periodic DFT Calculations and ab Initio Atomistic Thermodynamics. *The Journal of Physical Chemistry C,* 2014, **118**, 13667-13673.

2 Kowalski PM, Meyer B, Marx D. Composition, structure, and stability of the rutile-TiO_2(110)surface: Oxygen depletion, hydroxylation, hydrogen migration, and water adsorption. *Physical Review B,* 2009, **79**, 115410.

3 Wang S*, et al.* First principles studies of CO_2 and O_2 chemisorption on La_2O_3 surfaces. *Phys. Chem. Chem. Phys.,* 2017, **19**, 26799-26811.

4 Haj Lakhdar M, Smida YB, Amlouk M. Synthesis, optical characterization and DFT calculations of electronic structure of Sb_2O_3 films obtained by thermal oxidation of Sb2S3. *J. Alloys Compd.,* 2016, **681**, 197-204.

5 Yuan B, Koss AR, Warneke C, Coggon M, Sekimoto K, de Gouw JA. Proton-Transfer-Reaction Mass Spectrometry: Applications in Atmospheric Sciences. *Chem. Rev.,* 2017, **117**, 13187-13229.

6 Gandolfo A*, et al.* Unexpectedly High Levels of Organic Compounds Released by Indoor Photocatalytic Paints. *Environ. Sci. Technol.,* 2018, **52**, 11328-11337.